Rare Metal Materials and Engineering
Volume 52, Issue 7, July 2023
Available online at www.rmme.ac.cn

Science Press

Cite this article as: Jing Yunbing, Gan Chunlei, Miao Yupeng, et al. Microstructure Evolution and Properties of Continuous Columnar-Grained Polycrystalline Copper During Intense Plastic Deformation Process at Room Temperature[J]. Rare Metal Materials and Engineering, 2023, 52(07): 2364-2376.

ARTICLE

Microstructure Evolution and Properties of Continuous Columnar-Grained Polycrystalline Copper During Intense Plastic Deformation Process at Room Temperature

Jing Yunbing[1], Gan Chunlei[1], Miao Yupeng[1], Zhou Nan[1], Zhang Zhibo[2]

[1] Guangdong Provincial Key Laboratory for Technology and Application of Metal Toughening, Institute of New Materials, Guangdong Academy of Sciences, Guangzhou 510650, China; [2] Foshan Industrial Technology Research Institute, Guangdong Academy of Sciences, Foshan 528000, China

Abstract: The microstructure evolution and properties of continuous columnar-grained (CCG) polycrystalline copper during intense drawing deformation at room temperature were investigated by optical microscope, scanning electron microscope, Vickers microhardness tester, and universal tensile testing machine. The stored energy was calculated according to the structural parameters of dislocation cells in different textures based on high-resolution electron backscattered diffraction. Results show that CCG microstructure is gradually thinned into fibrous tissue. The as-cast CCG polycrystalline copper has tensile strength of 168 MPa, elongation of 52%, and conductivity of 103%IACS. After the drawing deformation of 99% at room temperature, the tensile strength of CCG polycrystalline copper increases to 455 MPa. However, the elongation reduces to 3%, and the conductivity decreases 96.8%IACS. Both the transverse and longitudinal sections of CCG polycrystalline copper have <001> original preferred orientation. A large number of fiber textures of <111> orientation and a small number of fiber textures of <001> orientation are formed with increasing the drawing deformation amount. Cube texture of the transverse section gradually decreases, and S texture and Copper texture gradually increase. Meanwhile, the Cube texture and Goss texture of longitudinal section are gradually transformed into Brass texture, Copper texture, and S texture. The kernel average misorientation (KAM) value at grain boundaries and in the deformation bands is large. Additionally, with increasing the deformation amount, KAM value is gradually increased and the stress is more concentrated. Under the same deformation conditions, the transverse section has higher stored energy than the longitudinal section does, and <001> orientation fiber texture has lower stored energy than <111> orientation fiber texture does. After the strong plastic deformation, CCG polycrystalline copper still has a large number of deformation textures with “soft” <001> orientation, which is an important reason for its low work hardening rate and excellent cold deformation ability.

Key words: continuous columnar grain; texture; stored energy

Continuous unidirectional solidification (CUS) process is an advanced casting technology, whose process contains the heating of molten liquid phase at the front side of solidification interface and simultaneously forced cooling of solidified solid phase. As a result, a unidirectional heat transfer environment is generated to promote the crystal growth against the direction of heat flow. Through the proper control of mold temperature, casting speed, and the amount of cooling water, the ingots with single crystal or continuous columnar-grained (CCG) polycrystalline structure can be obtained[1–2]. Compared with the ordinary polycrystalline materials prepared by conventional process, the ingot produced by continuous unidirectional solidification process has dense structure, and no casting defects, such as pores, shrinkage cavities, or shrinkage pores, occur, which reduces or even eliminates the intermediate annealing in the cold working process, thereby improving the production efficiency[3–6]. The excellent plasticity and ductility at room

Received date: November 14, 2022
Foundation item: Guangdong Academy of Sciences Projects (2020GDASYL-20200103133, 2020GDASYL-20200503001-03); Guangdong Province Science and Technology Plan Project (2014B070706027); Qingyuan Science and Technology Plan Project (2021SJXM030)
Corresponding author: Gan Chunlei, Ph. D., Senior Engineer, Institute of New Materials, Guangdong Academy of Sciences, Guangzhou 510650, P. R. China, E-mail: ganchunlei@163.com

temperature of continuous columnar polycrystalline are closely related to its microstructure characteristics. Gao et al[7] used optical microscope (OM) and transmission electron microscope (TEM) to study the microstructure of CCG copper during the drawing process, and found that CCG copper has no transverse grain boundaries. The characteristics of low angle grain boundaries as well as the development of dislocation cells and deformation twins along specific directions results in the excellent cold working deformability of CCG copper. Chen et al[8] measured the misorientation and spatial distribution of dislocation interfaces in CCG copper by electron backscattered diffraction (EBSD) and TEM, and reported that the primary columnar crystal structure affects the evolution and development of deformation substructure. It is also found that through the continuous evolution and refinement of deformed structures, the room-temperature extensive deformation of CCG copper can be conducted during the continuous strengthening process.

Currently, the process parameters of continuous unidirectional solidification to prepare single crystal copper wire have been widely studied. However, due to the restrictions of equipment and technology, single crystal copper wire must be plastically deformed before actual production. Therefore, in this research, CUS technique was used to prepare CCG pure copper rods with bright surface. The as-cast rod was then cold-drawn without heat treatment and the cumulative deformation amount reached 99%. The deformation mechanism of CCG copper in the drawing deformation process was studied, providing plastic deformation theory of CCG copper and theoretical basis for the development of high-strength and high-conductivity wires of ultra-fine copper and copper alloys.

1 Experiment

CCG copper rod with diameter of 8 mm was fabricated by 99.99wt% copper through CUS technique. Subsequently, the as-cast rod was cold-drawn with multi-passes at room temperature without intermediate annealing.

After 28 passes, the rod was drawn into the wire with 0.75 mm in diameter, and five pure copper wires were obtained with deformation amount of 0%, 30%, 60%, 90%, and 99%. The schematic diagram of transverse- and longitudinal-section specimens of pure copper wire with different deformation amounts is shown in Fig. 1. The drawing direction, normal direction, and transverse direction are represented by RD, ND, and TD, respectively.

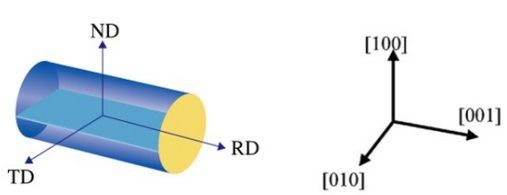

Fig.1 Schematic diagram of transverse- and longitudinal-section specimens of pure copper wire

All specimens were mechanically polished and then electropolished in the chemical solution (200 mL water+100 mL phosphoric acid+100 mL ethanol+20 mL isopropanol+2 g urea) at voltage of 5 V for 8 s. EBSD measurement was conducted by Gemini SEM300 with HKL Channel 5 analysis software. The operation voltage was 20 KV and the scanning step size was 0.02 – 0.2 μm. The microhardness of copper specimens was measured by HV-5 microhardness tester. The mechanical properties of the specimens were tested by a DNS-200 universal tensile machine, and the drawing speed was 2 mm/min. The conductivity of the specimen was measured by a QJ-36a DC numerical double-arm bridge tester.

2 Results and Discussion

2.1 Microstructure evolution

Fig. 2 shows the microstructure evolution of transverse and longitudinal sections of copper rod after drawing deformation of different amounts. When the drawing deformation amount is 0% (Φ=8.0 mm), the copper rod is composed of several columnar grains which are elongated along the solidification direction, and no transverse grain boundaries can be observed, as shown in Fig. 2a and 2f. During CUS process, the radial temperature gradient is very small, and the mold wall temperature is higher than the melting point of the metal. The nucleation and growth of molten metal in the mold wall and the formation of equiaxed crystals are inhibited. The solidification mainly dissipates the heat along casting direction, which promotes the growth of columnar grains[9–10]. When the deformation amount is 30% (Φ=6.8 mm), the original grains have no splits. The structures of transverse section are deformed by different compressive stresses and constant tensile stress during the drawing process, and the substructures inside the grains exhibit fiber stripe characteristics, as shown in Fig. 2b. The original longitudinal grain boundaries are obvious in the longitudinal section, and some deformation bands appear at a certain angle (45°) to RD in several zones. Some transition zones exist between the deformation bands, so the grains between the deformation zones rotate continuously to maintain the continuity of grain orientation. Most original columnar grains remain intact, and a few grains are elongated, as shown in Fig. 2g. When the deformation amount is 60% (Φ=5.0 mm), an obvious relative rotation occurs between different parts of the original grains in the transverse section, and a large number of deformed substructures lead to the difficult identification of original grain boundaries, as shown in Fig. 2c. The grains in longitudinal section are parallel to RD, and the grain boundaries are straight. It is also found that the deformation is relatively uniform, as shown in Fig.2h. Compared with Fig.2g, it can be seen that the angle between RD and the direction of deformation bands decreases, indicating that with increasing the drawing deformation amount, the orientation of deformed bands rotates towards RD[11–12]. When the deformation amount is 90% (Φ=2.7 mm), the strong plastic deformation at room temperature further enhances the microstructure difference between the transverse and longitudinal sections of CCG

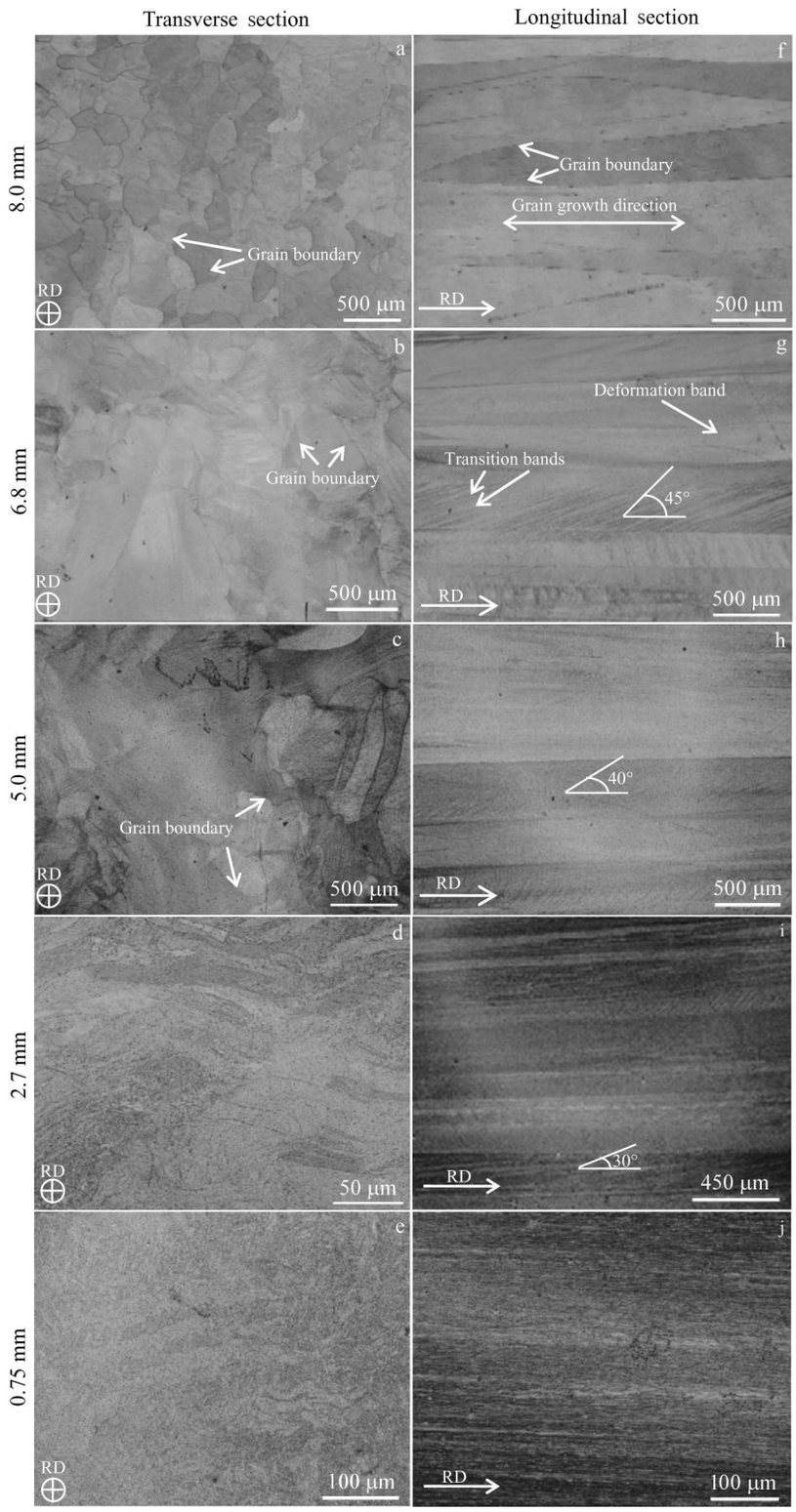

Fig.2 Microstructures of transverse (a–e) and longitudinal (f–j) sections of deformed copper rods with different diameters: (a, f) 8.0 mm; (b, g) 6.8 mm; (c, h) 5.0 mm; (d, i) 2.7 mm; (e, j) 0.75 mm

copper. Due to the uneven deformation, the grains in the entire transverse section present curled morphology, and the grain boundaries become indistinct. With increasing the drawing deformation amount, the grains in the longitudinal section are split, kinked, and fragmented. Many fiber stripes exist in the grains, and the angle between RD and the direction of deformation bands becomes smaller. The grains are in the form of extremely fine strips and fibers, as shown in Fig. 2d and 2i. When the deformation amount is 99% (Φ=0.75 mm), no grain boundaries can be observed in the cross section, and the grains along the longitudinal section are basically completely refined, forming the fiber tissue, as shown in

Fig. 2e and 2j. In conclusion, the cracking and fragmentation of grains and the inhomogeneity of deformation exist in the whole drawing process.

2.2 Texture analysis

In order to analyze the microstructure development and texture evolution during deformation, EBSD observation of the microstructure of CCG pure copper wires after deformation of different amounts was conducted.

Fig. 3 shows the inverse pole figures (IPFs) of transverse and longitudinal sections of the copper rod after deformation of different amounts. Fig. 4 and Fig. 5 show the corresponding grain size distributions, IPFs, and misorientation angle distributions of the transverse and longitudinal sections, respectively. With increasing the amount of drawing deformation, the grain size of transverse and longitudinal sections is decreased gradually. It can be seen that the average grain size of transverse section decreases from 1363 μm to 4.72 μm, and that of longitudinal section decreases from 3142 μm to 36 μm. CCG copper has <001> original preferred orientation along both TD and RD. With increasing the drawing deformation amount, the grain orientation changes from <001> direction into <111> direction. Finally, the grains are composed of <111>+<001> bi-oriented fiber textures, as shown in Fig. 4j and Fig. 5j. According to metal solidification theory, the grain growth rate is related to the crystal orientation. Copper has face-centered cubic (fcc) crystal structure, and its grain growth rate decreases sequentially along <001>, <110>, and <111> directions[13]. During the continuous casting process, the <001> orientation is consistent with the axial temperature gradient direction. The new grains nucleate and grow into columnar grains near <001> direction. With increasing the drawing deformation amount from 0% to 30%, the <001>-oriented texture is gradually transformed into <112>-dominated metastable texture, and the <111> orientation texture disappears. When the deformation amount further increases to 60%, a large amount of <111> texture forms and the <001> texture rapidly decreases. With the drawing process proceeding, the metastable textures are gradually transformed into the stable <111> texture, and some metastable textures are transformed back into <001> texture.

Fig. 4k–4o and Fig. 5k–5o show the distributions of misorientation angle between adjacent grains in the transverse and longitudinal sections, respectively. The frequency of misorientation angles in the transverse and longitudinal sections are shown in Table 1 and Table 2, respectively. It can be found that the transverse and longitudinal sections of the as-drawn copper wires always present the low angle boundary characteristics. When the deformation amount is 30%, the low angle grain boundaries account for 97.4% in the transverse section. When the drawing deformation amount is 99%, the high angle grain boundaries account for 24.5% in the transverse section. With increasing the drawing deformation amount, the proportion of low angle grain boundaries is gradually decreased, whereas that of large angle grain boundaries is increased. It can also be seen that the misorientation distribution becomes wider[14–16]. These phenomena are similar to those in the longitudinal sections. The proportion of low angle grain boundaries (<15°) decreases from 98.1% to 69.9%, and that of high angle grain boundaries increases significantly. It is suggested that after grain splitting, local shearing, and dynamic recovery, the large angle grain boundaries are generated in the form of deformation bands and dislocation interfaces in CCG copper[17–18].

Fig. 6 and Fig. 7 show the schematic diagrams of ideal orientations as well as the orientation distribution function (ODF) diagrams and EBSD maps of the transverse sections of copper rod under different deformation amounts, respectively. In order to simplify the analysis of orientation distribution of

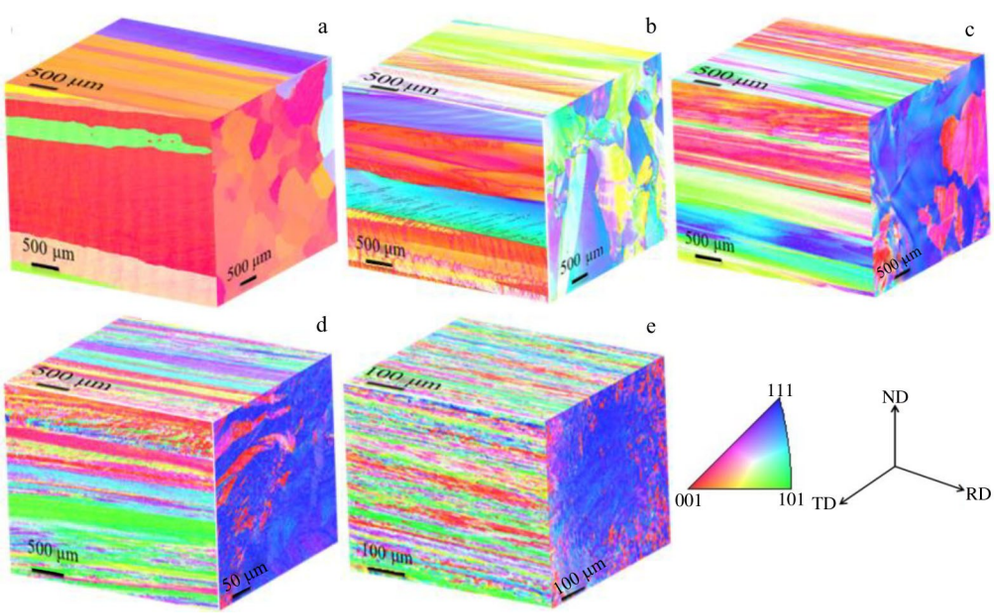

Fig.3 IPFs of transverse and longitudinal sections of copper rod after deformation of 0% (a), 30% (b), 60% (c), 90% (d), and 99% (e)

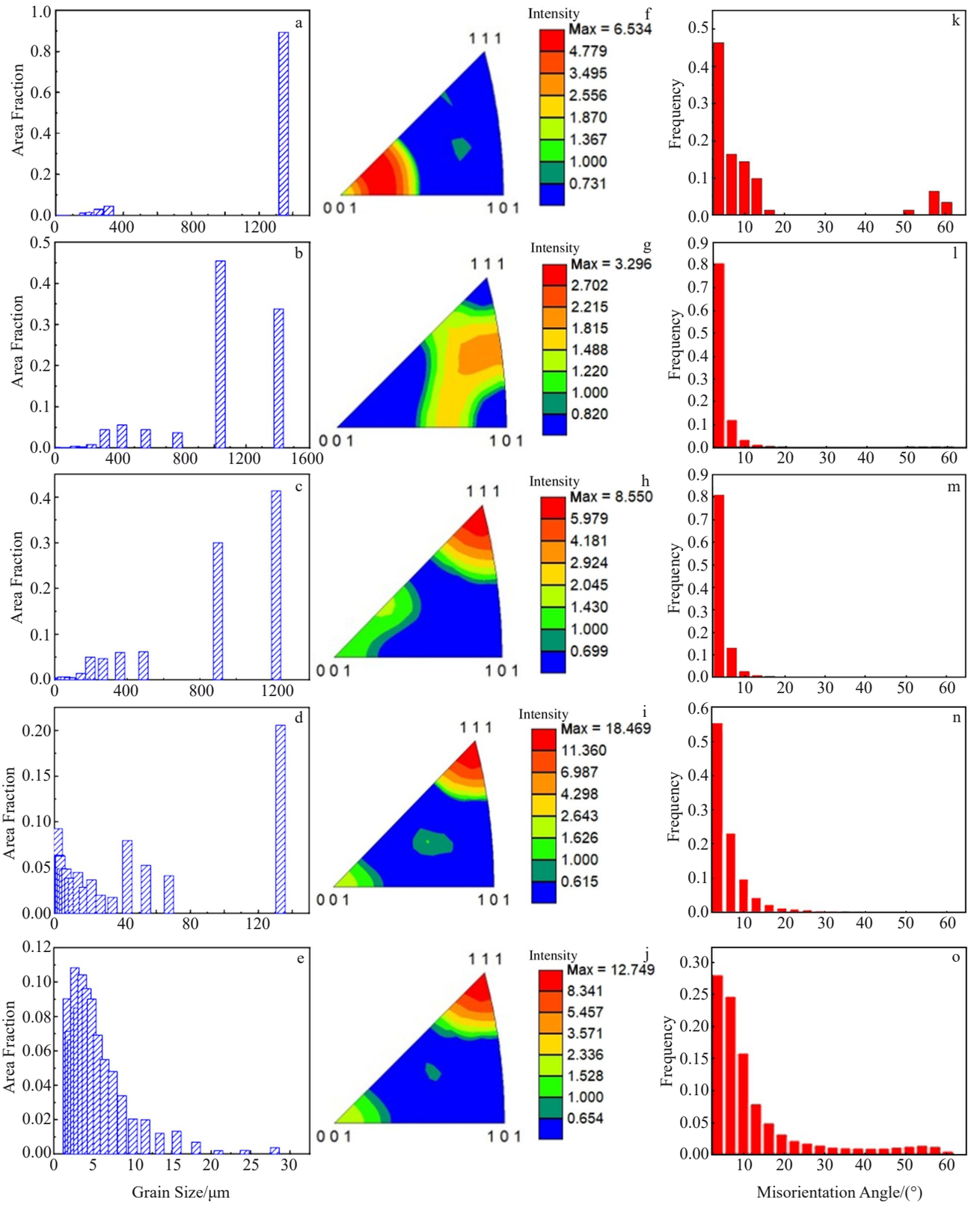

Fig.4 Grain size distributions (a – e), IPFs (f – j), and misorientation angle distributions (k – o) of transverse sections of copper rods after deformation of 0% (a, f, k), 30% (b, g, l), 60% (c, h, m), 90% (d, i, n), and 99% (e, j, o)

texture in Euler space, Fig.6 shows the ideal positions of main typical textures of fcc metal on ODF cross section at φ_2=0°, 45°, and 65° during drawing[19]. When the cold drawing deformation amount is 0%, the transverse section is mainly composed of Cube texture and a small amount of S texture. When the cold drawing deformation amount is 30%, the

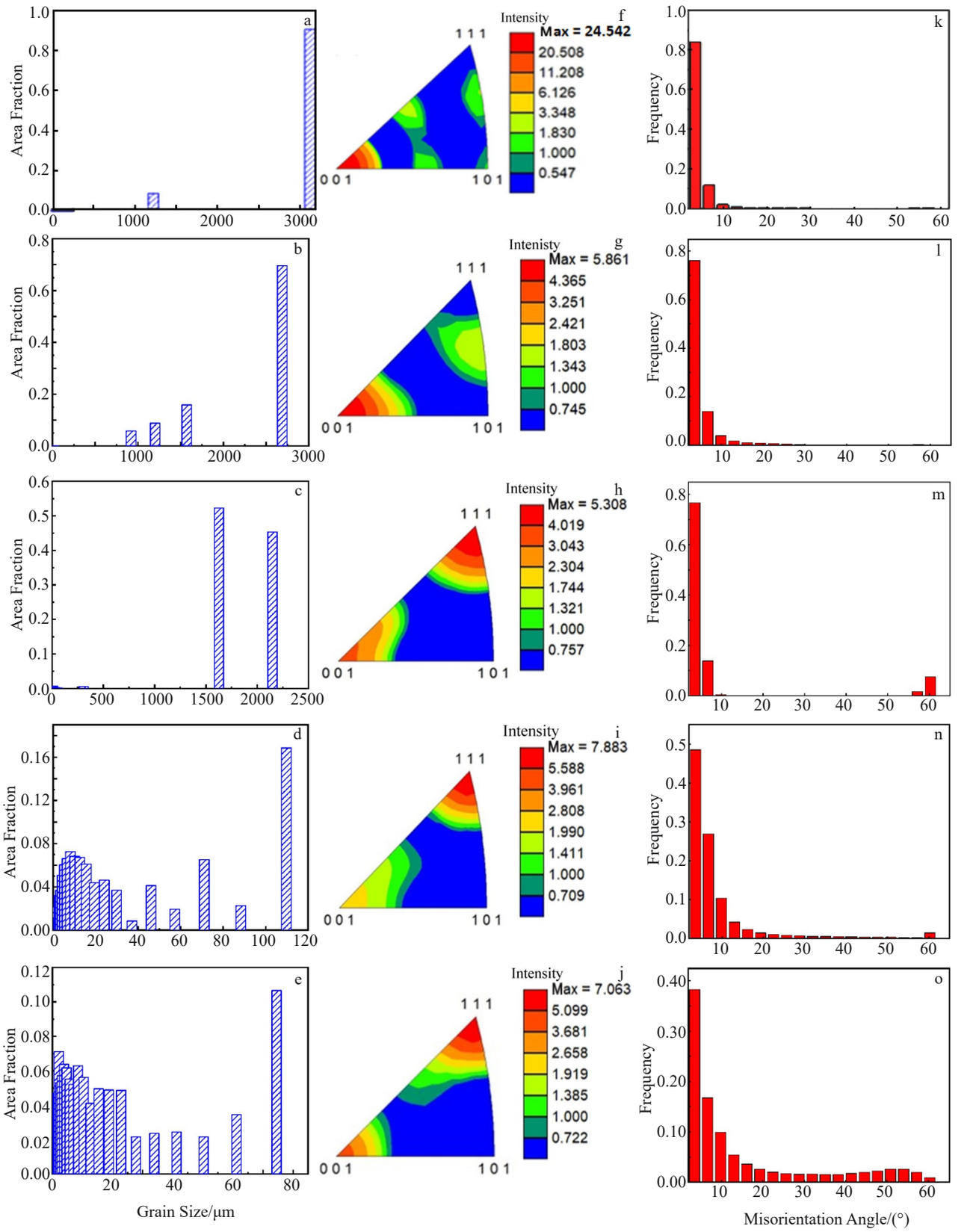

Fig.5 Grain size distributions (a–e), IPFs (f–j), and misorientation angle distributions (k–o) of longitudinal sections of copper rods after deformation of 0% (a, f, k), 30% (b, g, l), 60% (c, h, m), 90% (d, i, n), and 99% (e, j, o)

content of Cube texture decreases sharply, and the textures of transverse section are mainly Goss texture, Brass texture, and S texture. When the cold drawing deformation amount is 60%, Brass texture and Goss texture are reduced in the transverse section, and Cube texture can be observed. Besides, the content of S texture and Copper texture increases. Cube

Table 1 Frequency of misorientation angles of transverse section of copper rods after deformation (%)

Deformation amount	<5°	5°–10°	10°–15°	>15°
0	81.0	15.6	0.8	2.6
30	80.7	15.2	1.1	3.0
60	46.9	35.8	4.4	12.9
90	45.2	39.2	4.9	10.7
99	28.0	40.5	7.0	24.5

Table 2 Frequency of misorientation angles of longitudinal section of copper rods after deformation (%)

Deformation amount	<5°	5°–10°	10°–15°	>15°
0	84.0	13.5	0.6	1.9
30	81.1	13.3	1.3	4.3
60	77.6	12.2	1.0	9.2
90	48.5	37.2	4.2	10.1
99	38.2	26.7	5.0	30.1

texture, S texture, and Copper texture are the main texture types. When the drawing deformation amount exceeds 90%, the microstructure is further refined, the content of Cube texture continues to decrease, and the content of S texture and Copper texture barely changes. A small amount of Goss texture and Brass texture still exists in the transverse section, but their texture strength is low.

With increasing the drawing deformation amount, the textures of longitudinal section are also changed. Fig. 8 and Fig. 9 show the schematic diagrams of ideal orientations as well as ODF diagrams and EBSD maps of the longitudinal section of copper rod under different deformation amounts, respectively. In the as-cast state, the longitudinal section is only composed of Cube texture and a small amount of Goss texture. When the deformation amount of copper rod increases to 30%, although the longitudinal section is still composed of Cube texture and Goss texture, the content of Cube texture significantly reduces, whereas the proportion of Goss texture increases rapidly. When the cold drawing deformation amount is 60%, the Cube texture and Copper texture increase significantly, a certain amount of Goss texture exists in the deformed copper, and other typical textures are gradually transformed into typical fcc texture types[20]. When the drawing deformation amount is 90%, a small amount of Brass

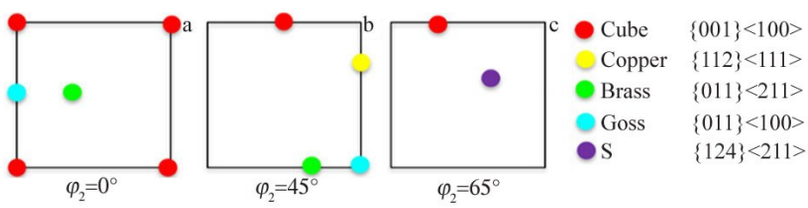

Fig.6 Schematic diagrams of ideal orientations in transverse section of as-rolled fcc material at φ_2=0° (a), φ_2=45° (b), and φ_2=65° (c)

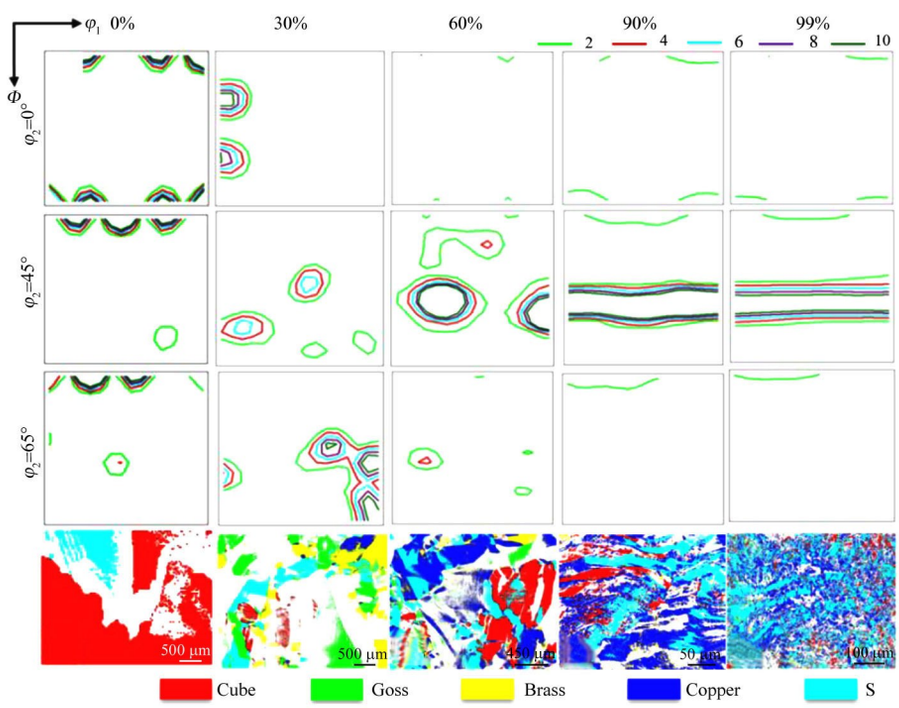

Fig.7 ODF diagrams and EBSD maps of textures in transverse section of room-temperature CCG copper under different deformation amounts

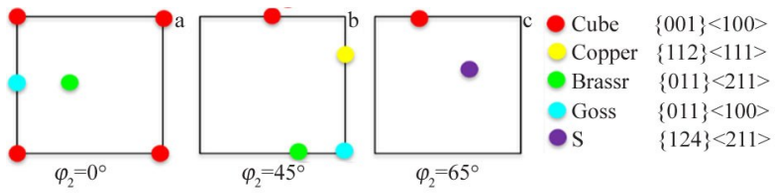

Fig.8 Schematic diagrams of ideal orientations in longitudinal section of as-rolled fcc material at φ_2=0° (a), φ_2=45° (b), and φ_2=65° (c)

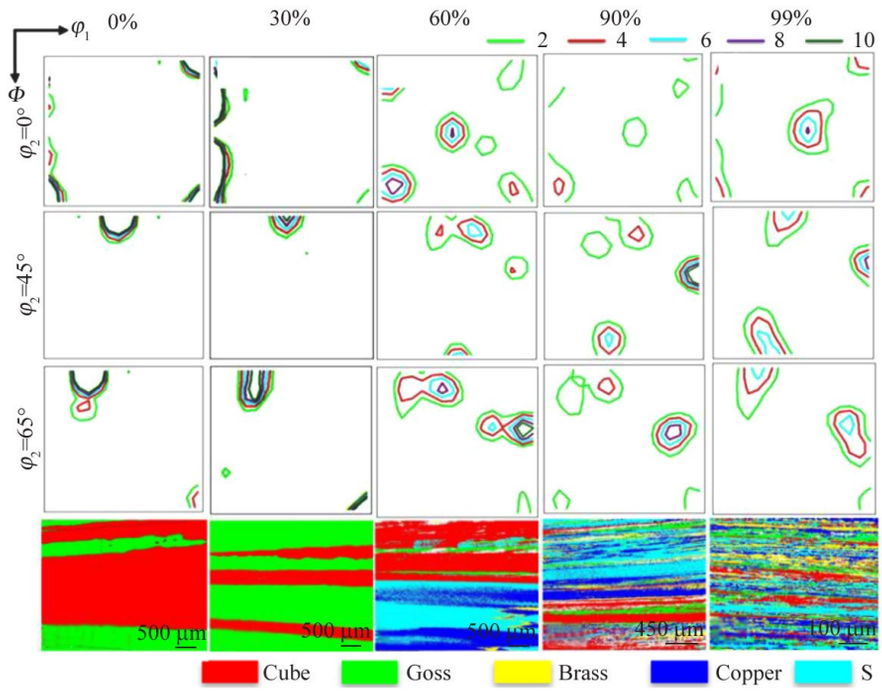

Fig.9 ODF diagrams and EBSD maps of textures in longitudinal section of room-temperature CCG copper under different deformation amounts

texture can be observed, and the Goss texture content hardly changes. Meanwhile, the longitudinal section is mainly composed of Cube texture, S texture, and Copper texture. With further increasing the deformation amount to 99%, it can be observed that there are five typical textures distributed along RD.

2.3 Mechanical properties

Mechanical properties of CCG pure copper rod under different drawing deformation amounts are evaluated by microhardness tests and uniaxial tensile tests, and the results are shown in Fig. 10. It can be observed that with increasing the drawing deformation amount, the microhardness of pure copper wire is increased from 490 MPa to 1166 MPa, which is improved by 138% due to the work hardening effect. When the drawing deformation amount is 0% – 30%, the microhardness rises sharply. However, when the drawing deformation amount is 30% – 99%, the microhardness increment gradually decreases.

When the drawing deformation amount is 0%, the ultimate tensile strength of CCG copper is 168 MPa, and the yield strength is 88 MPa. Additionally, the elongation reaches a peak value of 52%. It can be found that when the drawing deformation amount is 0%–90%, the ultimate tensile strength and yield strength increase rapidly, whereas the elongation decreases significantly. Nevertheless, when the deformation amount is 90%–99%, both the ultimate tensile strength and yield strength increase slowly, suggesting that CCG copper can be continuously hardened but at a low work hardening rate. When the drawing deformation amount is 99%, the ultimate tensile strength reaches 455 MPa, which is 2.7 times higher than that of the as-cast copper. Besides, the yield strength increases to 448 MPa, and the elongation decreases to 3%.

CCG copper produces multisystem slip during plastic deformation. Dislocations move along the glide plane and form dislocation forest at the grain boundaries, thereby increasing the dislocation density. Moreover, the interaction of dislocations in different slip systems results in the entanglement of dislocations, and thus the resistance against dislocation movement is improved, leading to the work hardening and sharp increase in microhardness. With further increasing the drawing deformation, the dynamic recovery occurs in the grains, and the dislocation network is straight

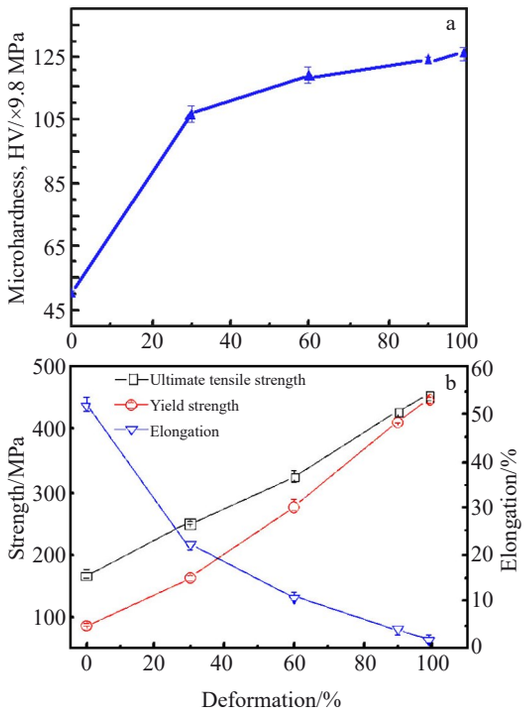

Fig.10 Microhardness (a) and tensile properties (b) of CCG copper under different deformation amounts

and regular through cross-slip and climbing, forming low-angle dislocation interfaces, sub-grain boundaries, lamellar dislocation interfaces, and deformation twin[21]. In this case, the microhardness increases slowly. Moreover, the grain refinement can result in a significant increase in the total area of grain boundaries, leading to difficult dislocation slip. It is considered that the dual effects of work hardening and fine grain strengthening lead to the increase in microhardness[22]. The substructure produced at the initial stage of deformation also plays an important role in strengthening effect: it causes the rapid increase in tensile strength and quick decrease in elongation[23]. After the dislocations are piled up to a certain extent, a layered interface is formed, and the dislocations with different signs are gradually offset by the merger between the dislocation interfaces until balance[24], resulting in the slow increase in tensile strength and basically unchanged elongation.

2.4 Conductivity

Fig. 11 illustrates the conductivities of CCG copper rods under different deformation amounts. When the deformation amount increases from 0% to 99%, the conductivity decreases from 103%IACS to 96.8%IACS. During the cold drawing process, although the stress concentration generated inside the grain does not destroy the lattice integrity, it will change the lattice constant of crystal, distort the lattice periodicity, and increase the probability of electron scattering. Meanwhile, the pure copper deformed by cold drawing can produce crystal defects, such as microscopic cracks and voids. These defects tend to accumulate with the deformation proceeding, resulting

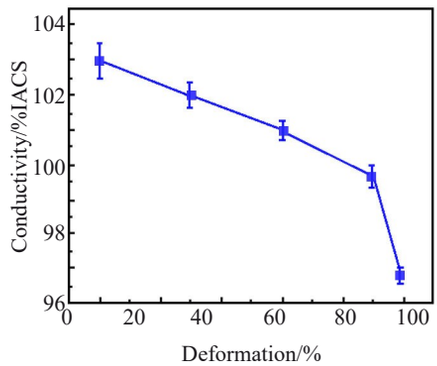

Fig.11 Conductivity of CCG copper rods under different drawing deformation amounts

in the increase in electrical resistance. Thus, the conductivity decreases. However, CCG pure copper only has a small number of longitudinal grain boundaries, which is the main reason for its excellent electrical conductivity even after drawing deformation of 99%.

2.5 Kernel average misorientation

The level of metal plastic deformation can be quantitatively estimated by the change in kernel average misorientation (KAM). EBSD can be used to calculate the average angular misorientation between adjacent scanning points. Different colors in KAM diagram represent different levels of strain concentration, reflecting the plastic deformation capacity in the grains and at grain boundaries.

Fig.12 displays KAM images of transverse and longitudinal sections of copper rod under different deformation amounts. It can be found that the bright color is concentrated at the grain boundaries, indicating that the strain concentration is large. With increasing the drawing deformation amount, the dislocations near the grain boundaries are more concentrated. This is because adjacent grains will restrict each other in order to coordinate the deformation, resulting in stress concentration. KAM is increased with increasing the deformation amount, implying that the number of deformed sub-grains is increased significantly. Therefore, the number of grain boundaries hindering the dislocation movement increases, and greater applied stress is required to activate dislocations. In addition, KAM in the area affected by grain boundary changes obviously, particularly at the junction of slip band (black circle part in Fig.12g).

In order to explain the stress concentration at grain boundaries, the misorientation in or between grains (black square part in Fig.12b) is measured, and the results are shown in Fig.13. The misorientation within the grain (point A to point C) is <2°, and the misorientation at the grain boundary (point A to point B) is approximately 40°. The crystal orientations between adjacent grains are different, and the critical shear stresses of different slip systems are also different. The slip firstly occurs in the grains with “soft orientation”, and the dislocations move in a certain direction along the slip plane.

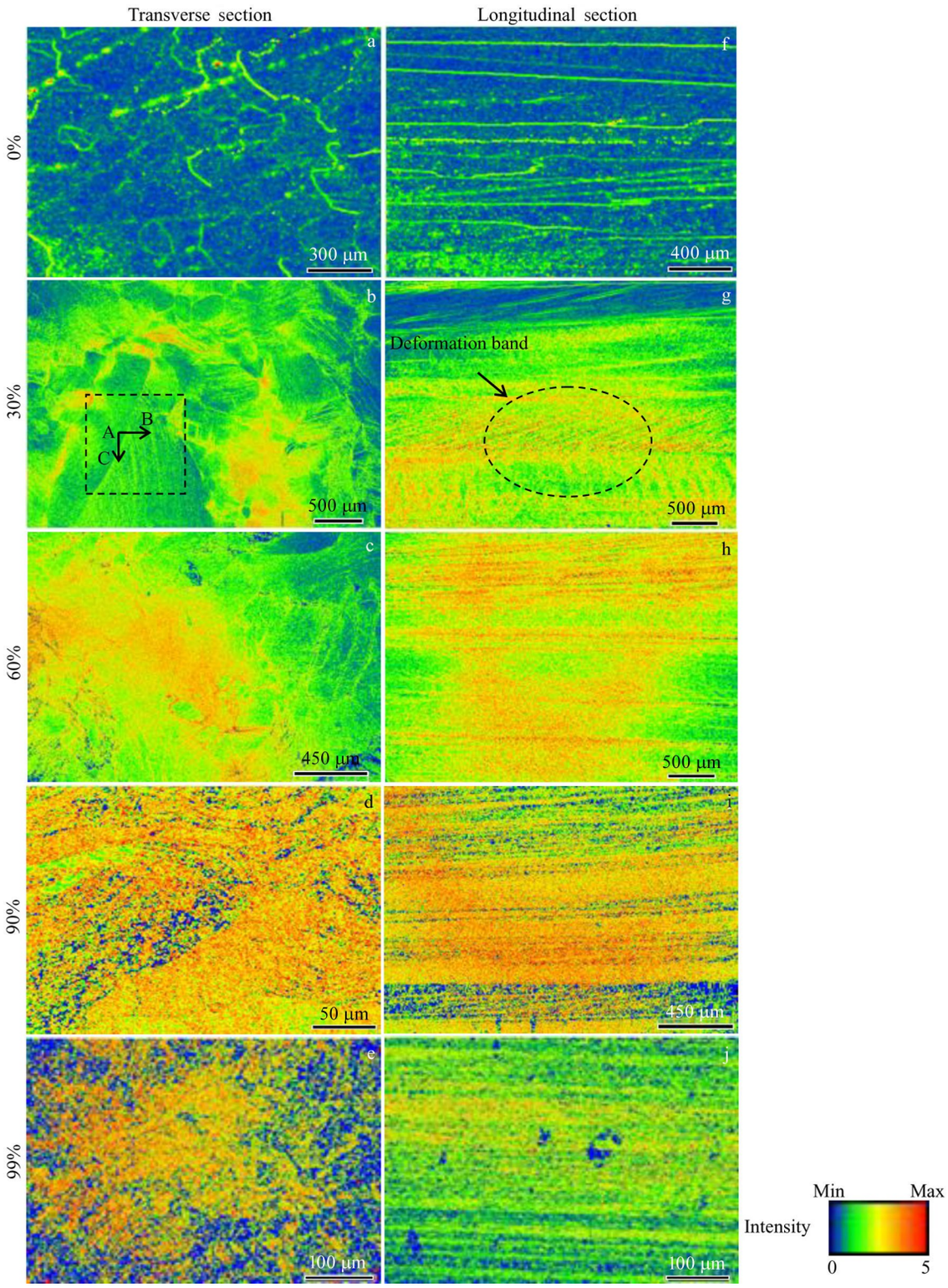

Fig.12 KAM images of transverse (a–e) and longitudinal (f–j) sections of CCG copper rods after deformation of 0% (a, f), 30% (b, g), 60% (c, h), 90% (d, i), and 99% (e, j)

However, the surrounding grains with "hard orientation" do not satisfy the critical conditions for shear stress. Thus, the dislocations cannot move across the grain boundaries, and the slip cannot be transmitted to adjacent grains. In order to achieve continuous deformation, some crystals will rotate or kink relatively to other parts, resulting in folds and forming a place for local stress concentration near the grain boundary[25].

2.6 Stored energy calculation

It is well known that the energy is stored in the material in the form of dislocations during plastic deformation. In this research, high resolution EBSD was used to measure the shape, size, and spatial distribution of dislocation cells, and

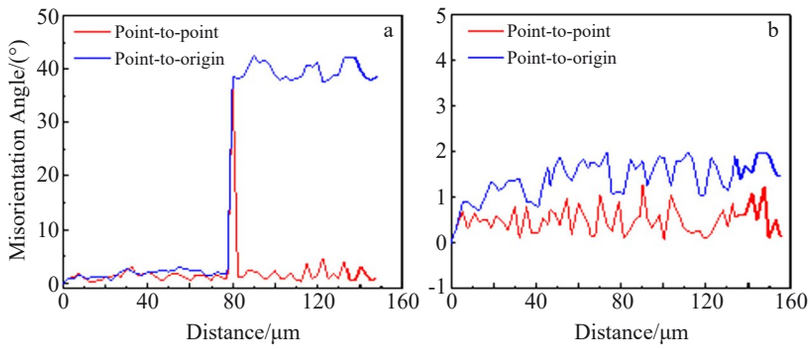

Fig.13 Misorientation angle distributions from point A to point B (a) and from point A to point C (b) in Fig.12b

the microstructure parameters were analyzed.

It is found that the grain boundary energy (GBE) per unit area is related to the misorientation angle across the boundaries, which can be expressed by the Read-Shockley equation[26–27], as follows:

$$J_i^j = \begin{cases} J\dfrac{\theta_i^j}{\theta^m}\left[1 - \ln\dfrac{\theta_i^j}{\theta^m}\right] & \theta_i^j < \theta^m \\ J & \theta_i^j \geqslant \theta^m \end{cases} \quad (1)$$

where J is GBE per unit area (for copper, J=0.625 J/m^2), θ_i^j is the boundary misorientation angle, and θ^m is 15°.

The stored energy per unit volume (E_S) caused by the dislocation boundary of misorientation angle can be obtained by calculation related to the total grain boundary area per unit volume (S_V), as follows:

$$E_S = E(\rho_0) + \int S_V J \mathrm{d}S = \bar{J}S_V + E(\rho_0) \quad (2)$$

where $E(\rho_0)$ is the contribution of individual dislocation to the stored energy in the dislocation boundaries, which can be neglected; $\bar{J}$ is the average GBE per unit area, and it is determined by the distribution of misorientation angle of the dislocation boundaries; S is the grain boundary area.

The total grain boundary area per unit volume S_V is related to the average boundary spacing (d), which can be expressed by Eq.(3), as follows:

$$S_V = f/d \quad (3)$$

where f is a dimensionless parameter related to the grain geometry. Assuming that all dislocation cells are fully equiaxed, the value of parameter f is 2.

Substituting Eq.(3) into Eq.(2), Eq.(4) can be obtained, as follows:

$$E_S = \bar{J}f/d \quad (4)$$

The value of average spacing d was estimated by EBSD, the average GBE per unit area $\bar{J}$ was calculated by Eq.(1), and the stored energy E_S of transverse and longitudinal sections was calculated by each texture based on EBSD measurement, as listed in Table 3 and Table 4, respectively. It can be found that the stored energy is increased with increasing the drawing

Table 3 Stored energy of transverse section of CCG pure copper based on EBSD measurement

Deformation amount/%	$\bar{J}$/J·m^{-2}	<001> fiber texture		<111> fiber texture		Other fiber textures	
		d/μm	E_S/MJ·m^{-3}	d/μm	E_S/MJ·m^{-3}	d/μm	E_S/MJ·m^{-3}
0	0.19	1.523	0.250	-	-	-	-
30	0.26	1.279	0.407	-	-	0.639	0.814
60	0.32	0.902	0.710	0.227	2.819	0.410	1.561
90	0.38	0.467	1.627	0.187	4.064	0.249	3.052
99	0.42	0.315	2.667	0.124	6.774	0.198	4.242

Table 4 Stored energy of longitudinal section of CCG pure copper based on EBSD measurement

Deformation amount/%	$\bar{J}$/J·m^{-2}	<001> fiber texture		<111> fiber texture		Other fiber textures	
		d/μm	E_S/MJ·m^{-3}	d/μm	E_S/MJ·m^{-3}	d/μm	E_S/MJ·m^{-3}
0	0.21	3.128	0.134	-	-	-	-
30	0.29	2.439	0.237	-	-	1.082	0.569
60	0.36	1.272	0.566	0.498	1.446	0.831	0.866
90	0.47	0.925	1.016	0.304	3.092	0.469	2.004
99	0.53	0.617	1.718	0.271	3.911	0.392	2.704

deformation amount. Under the same drawing deformation amount, the transverse section has higher stored energy than the longitudinal section does. The <001> texture has lower stored energy, and it is increased slowly with increasing the deformation, suggesting a slow work hardening rate. However, the <111> texture has higher stored energy, and it is increased rapidly with increasing the deformation amount, inferring that the <111> texture in dislocation cells can produce large strain and the work hardening rate is higher than that caused by other textures. CCG copper has a large number of <001> "soft" orientation textures under the same deformation amount, which is an important reason for its excellent ductility at room temperature.

3 Conclusions

1) During the drawing deformation of continuous columnar polycrystalline copper at room temperature, continuous columnar-grained (CCG) microstructure is gradually thinned down into fibrous tissue. The number of grains and the degree of deformation of the microstructure are increased with increasing the drawing deformation amount. The cracking and fragmentation of grains and the inhomogeneity of deformation exist in the whole drawing process.

2) CCG copper has preferred orientation of <100> along both the drawing direction and transverse direction. With increasing the drawing deformation amount, a large number of <111>-oriented textures and a small number of <001> -oriented textures are generated. Meanwhile, the proportion of low angle grain boundaries (<15°) decreases from 98.1% to 69.9%, and that of large angle grain boundaries increases significantly in the longitudinal section of CCG copper.

3) When the drawing deformation amount is 0%, the transverse and longitudinal sections are mainly composed of a large amount of Cube texture. With increasing the drawing deformation amount, the content of Cube texture is gradually decreased in the transverse section, whereas the content of S texture and Copper texture is gradually increased. The Cube texture and Goss texture in the longitudinal section are gradually transformed into Brass texture, Copper texture, and S texture. These five textures are scattered along the drawing direction.

4) With increasing the drawing deformation amount from 0% to 99%, the hardness of CCG copper is enhanced from 490 MPa to 1166 MPa, the tensile strength is increased from 168 MPa to 455 MPa, the elongation is decreased from 52% to 3%, and the conductivity is reduced from 103%IACS to 96.8%IACS.

5) CCG pure copper has high kernel average misorientation (KAM) value near the grain boundary and deformation zone. With increasing the deformation amount, KAM value is gradually increased, and the stress is more concentrated. Under the same deformation amount, the transverse section has higher stored energy than the longitudinal section does, and the <001> texture has lower stored energy than the <111> texture does.

References

1 Ohno A. *Journal of Metals*[J], 1986, 38(1): 14

2 Zhang L G, Song Q M, Xu X W *et al. Waste Management*[J], 2021, 124(4): 94

3 Li Fulin, Tan Haibing, Meng Lingchao *et al. Chinese Journal of Rare Metals*[J], 2020, 44(8): 807 (in Chinese)

4 Zhu X F, Xiao Z, An J H *et al. Journal of Alloys and Compounds*[J], 2021, 883: 160 769

5 Wu Heng, Zhang Hong, Lu Jiafeng *et al. The Chinese Journal of Nonferrous Metals*[J], 2017, 27(12): 2426 (in Chinese)

6 Fashu S, Khan R. *Engineering Science and Technology*[J], 2016, 19(4): 2100

7 Gao K W, Liu M Y, Zou F L *et al. Materials Science and Engineering A*[J], 2010, 527(18–19): 4750

8 Chen Jian, Yan Wen, Miao Jian *et al. Rare Metal Materials and Engineering*[J], 2011, 40(10): 1727 (in Chinese)

9 Xu Z M, Guo Z Q, Li J G. *Materials Characterization*[J], 2004, 53(5): 395

10 Zhang H, Xie J X, Wang Z D. *Journal of University of Science and Technology Beijing*[J], 2004, 11(3): 240

11 Kuhlmann W D. *Acta Materialia*[J], 1999, 47(6): 1697

12 Wulff F, Breach C D, Dittmer K. *Journal of Materials Science Letters*[J], 2003, 22(19): 1373

13 Paul H, Driver J H, Maurice C *et al. Materials Science and Engineering A*[J], 2003, 359(1): 178

14 Chen J, Yan W, Ding R G *et al. Journal of Materials Science*[J], 2009, 44(8): 1909

15 Wang Y, Huang H Y, Xie J X. *Materials Science and Engineering A*[J], 2011, 530: 418

16 Hanazaki K, Shigeiri N, Tsuji N. *Materials Science and Engineering A*[J], 2010, 527(21): 5699

17 Wang Y, Zhao H J. *Journal of Materials Engineering and Performance*[J], 2019, 28(3): 1884

18 Suresh K S, Subhasis S, Abhishek C *et al*. *Materials Characterization*[J], 2012, 70: 74

19 Zhang P, Wang H, Yao S J. *Metals and Materials International*[J], 2021, 27(2): 392

20 Lapeire L, Sidor J, Verleysen P. *Acta Materialia*[J], 2015, 95: 224

21 Li Yi, Zhang Xiangkai, He Kejian *et al. The Chinese Journal of Nonferrous Metals*[J], 2016, 26(1): 66 (in Chinese)

22 Song Kexing, Zhou Yanjun, Mi Xujun *et al. The Chinese Journal of Nonferrous Metals*[J], 2020, 30(12): 2845 (in Chinese)

23 Wang Lujuan, Song Kexing, Wang Qing *et al*. *Journal of Henan University of Science &Technology* (*Natural Science*) [J], 2013, 34(3): 14 (in Chinese)

24 Hughes D A, Hansen N. *Acta Materialia*[J], 2000, 48(11): 2985

25 Yin Wenhong, Wang Weiguo, Fang Xiaoying *et al. Journal of Shanghai University* (*Natural Science*) [J], 2017, 23(3): 414 (in Chinese)

26 Knudsen T, Cao W Q, Godfrey A *et al. Metallurgical and*

Materials Transactions A[J], 2008, 39(2): 430

Transactions A[J], 2005, 36(9): 2371

27 Godfrey A, Cao W Q, Liu Q *et al. Metallurgical and Materials*

连续柱状多晶铜室温强塑性变形过程中的微观组织演变和性能

敬云兵[1]，甘春雷[1]，苗钰鹏[1]，周　楠[1]，张志波[2]

(1. 广东省科学院 新材料研究所 广东省金属强韧化技术与应用重点实验室，广东 广州 510650)

(2. 广东省科学院 佛山产业技术研究院，广东 佛山 528000)

摘　要：利用光学显微镜、扫描电子显微镜、维氏显微硬度计和万能拉伸试验机，定量研究了连续柱状多晶铜在室温下强塑性拉拔变形过程中的组织演变和性能变化规律，并根据高分辨率电子背散射衍射技术测量的不同织构中位错胞的结构参数计算了形变储能。结果表明，连续柱状晶组织逐步细化为纤维晶组织，铸态连续柱状多晶铜的抗拉伸强度为168 MPa，延伸率为52%，导电率达到103%IACS。室温连续拉拔变形达到99%时，抗拉伸强度增加至455 MPa，延伸率下降至3%，导电率降低至96.8%IACS；连续柱状多晶铜的横截面和纵截面均具有<001>原始择优取向，且随着拉拔变形量的增加，最终形成大量的<111>取向+少量的<001>取向纤维织构。横截面中Cube织构逐渐减少，S织构和Copper织构逐渐增加，而纵截面中Cube织构和Goss织构逐渐向Brass织构、Copper织构和S织构转变。晶界和变形带处的核平均误差（KAM）值较高，且随着变形量的增加，KAM值逐渐增大，应力更集中。相同变形量下，横截面比纵截面具有更高的形变储能，<001>取向织构组分具有比<111>取向织构组分更低的形变储能。在大变形量加工之后，连续柱状多晶铜仍具有高含量的“软”取向<001>形变织构，是其具有低加工硬化率和优异的冷变形能力的重要原因。

关键词：连续柱状晶；织构；形变储能

作者简介：敬云兵，女，1993年生，硕士，广东省科学院新材料研究所广东省金属强韧化技术与应用重点实验室，广东 广州 510650，E-mail：jingyunbing@163.com